BRAIN
ORIGINAL ARTICLE

Phospho-tau with subthreshold tau-PET predicts increased tau accumulation rates in amyloid-positive individuals

Colin Groot,[1,2] Ruben Smith,[1,3] Erik Stomrud,[1,4] Alexa Pichet Binette,[1] Antoine Leuzy,[1] Anika Wuestefeld,[1] Laura E. M. Wisse,[5] Sebastian Palmqvist,[1,4] Niklas Mattsson-Carlgren,[1,3,6] Shorena Janelidze,[1] Olof Strandberg,[1] Rik Ossenkoppele[1,2,†] and Oskar Hansson[1,4,†]

[†]These authors contributed equally to this work.

Different tau biomarkers become abnormal at different stages of Alzheimer's disease, with CSF phospho-tau typically becoming elevated at subthreshold levels of tau-PET binding. To capitalize on the temporal order of tau biomarker-abnormality and capture the earliest changes of tau accumulation, we implemented an observational study design to examine longitudinal changes in tau-PET, cortical thickness and cognitive decline in amyloid-β-positive individuals with elevated CSF p-tau levels (P+) but subthreshold Tau-PET retention (T–). To this end, individuals without dementia (i.e. cognitively unimpaired or mild cognitive impairment, $n = 231$) were selected from the BioFINDER-2 study. Amyloid-β-positive (A+) individuals were categorized into biomarker groups based on cut-offs for abnormal CSF p-tau$_{217}$ and ^{18}F-RO948 (Tau) PET, yielding groups of tau-concordant-negative (A+P–T–; $n = 30$), tau-discordant (i.e. A+P+T–; $n = 48$) and tau-concordant-positive (A+P+T+; $n = 18$) individuals. In addition, 135 amyloid-β-negative, tau-negative, cognitively unimpaired individuals served as controls. Differences in annual change in regional tau-PET, cortical thickness and cognition between the groups were assessed using general linear models, adjusted for age, sex, clinical diagnosis and (for cognitive measures only) education. Mean follow-up time was ~2 years. Longitudinal increase in tau-PET was faster in the A+P+T– group than in the control and A+P–T– groups across medial temporal and neocortical regions, with the highest accumulation rates in the medial temporal lobe. The A+P+T– group showed a slower rate of increase in tau-PET compared to the A+P+T+ group, primarily in neocortical regions. We did not detect differences in yearly change in cortical thickness or in cognitive decline between the A+P+T– and A+P–T– groups. The A+P+T+ group, however, showed faster cognitive decline compared to all other groups. Altogether, these findings suggest that the A+P+T– biomarker profile in persons without dementia is associated with an isolated effect on increased tau-PET accumulation rates but not on cortical thinning and cognitive decline. While this suggests that the tau-discordant biomarker profile is not strongly associated with short-term clinical decline, this group does represent an interesting population for monitoring the effects of interventions with disease-modifying agents on tau accumulation in early Alzheimer's disease, and for examining the emergence of tau aggregates in Alzheimer's disease. Further, we suggest updating the AT(N) criteria for Alzheimer's disease biomarker classification to APT(N).

1 Clinical Memory Research Unit, Department of Clinical Sciences in Malmö, Lund University, 205 02 Malmö, Sweden
2 Alzheimer Center, Amsterdam UMC Location Vumc, 1081 HV Amsterdam, The Netherlands
3 Department of Neurology, Skåne University Hospital, Lund University, 222 42 Lund, Sweden
4 Memory Clinic, Skåne University Hospital, 222 42 Malmö, Sweden
5 Department of Diagnostic Radiology, Lund University, 223 62 Lund, Sweden
6 Wallenberg Center for Molecular Medicine, Lund University, 223 62 Lund, Sweden

Received April 05, 2022. Revised August 18, 2022. Accepted August 20, 2022. Advance access publication September 9, 2022

Correspondence to: Colin Groot, PhD
Memory Clinic, Skåne University Hospital, SE-205 02 Malmö, Sweden
E-mail: colin.groot@med.lu.se

Correspondence may also be addressed to: Oskar Hansson, MD, PhD
E-mail: oskar.hansson@med.lu.se

Keywords: Alzheimer; tau; PET; CSF; discordance

Introduction

Alzheimer's disease is characterized by two pathological hallmarks: amyloid-β plaques, and neurofibrillary tangles and neuropil threads consisting of hyperphosphorylated tau protein.[1,2] Amyloid-β pathology is thought to initiate the Alzheimer's disease pathological cascade while tau pathology is more closely linked to neurodegeneration and cognitive impairment.[3,4] Over the last decades, enormous resources have been dedicated to targeting amyloid-β to prevent the initiation of the Alzheimer's disease pathological cascade. Recently, more tau-focused Alzheimer's disease treatments are emerging, facilitated by recent biomarker developments for *in vivo* detection of tau pathology.[2]

In CSF, phosphorylated tau (p-tau) is specifically elevated in Alzheimer's disease,[2] and CSF p-tau levels are predictive of future cognitive decline.[5] In addition to CSF measures, tau pathology can now also be quantified and visualized *in vivo* using PET. Tau-PET has been shown to accurately differentiate between Alzheimer's disease and controls, and increases in tau-PET signal are associated with (longitudinal changes in) atrophy and cognitive decline across all stages of Alzheimer's disease.[6] In the AT(N) Alzheimer's disease biomarker classification system proposed in the National Institute on Aging–Alzheimer's Association (NIA-AA) Research Framework,[7] tau positivity can be defined by either biofluid measures of p-tau or by tau-PET, suggesting that CSF p-tau and tau-PET are interchangeable for measuring the presence of tau pathology. However, important differences in what aspects of tau-pathology CSF and PET represent have been identified.[8–10] CSF p-tau measures soluble variants of tau[11] and has been shown to be sensitive to the earliest tau changes in Alzheimer's disease.[12] On the other hand, tau-PET ligands bind aggregated, insoluble paired helical filaments of tau[13,14] reflecting the pathological accumulation of tau aggregates,[15] and tau-PET shows particular sensitivity to tau pathology in later stages of Alzheimer's disease. In line with these findings, recent investigations into the temporal relationship between CSF and PET revealed that CSF p-tau generally becomes abnormal before tau-PET.[15–17] This indicates that elevated CSF p-tau in combination with subthreshold levels of tau-PET is a sign of emerging Alzheimer's disease pathology, and individuals with this biomarker profile could be an interesting target group for intervention, and study population to map the earliest tau accumulation in Alzheimer's disease.

By implementing a multi-modal approach to split the 'T' category from the AT(N) Alzheimer's disease biomarker classification into CSF p-tau ('P') and tau-PET ('T') categories, capitalizing on the relative merits of these biomarkers, the present study aims to identify amyloid-β-positive (A+), tau-discordant (A+P+T–) cases among individuals without dementia (cognitively unimpaired or with mild cognitive impairment). Multi-modal investigations combining CSF and PET measurements of amyloid-β have revealed important clinical implications for discordance[17–20] and, given the close relationship between tau pathology, neurodegeneration and clinical symptoms, we hypothesize that the A+P+T– biomarker profile also has clinical, as well as neurobiological, implications. Specifically, we hypothesize that the A+P+T– group represents a biomarker profile that predicts future progression of Alzheimer's disease, including increases in tau accumulation, cortical thinning and cognitive decline.

Materials and methods

Participants

Participants were part of the Swedish BioFINDER-2 cohort (NCT03174938). BioFINDER-2 is a prospective, longitudinal study that focuses on identifying key mechanisms and improvement of diagnostics in Alzheimer's disease and other neurodegenerative disorders. For details about study design and methods see Leuzy *et al.*[21] and Palmqvist *et al.*[22] As our primary focus lay in the assessment of longitudinal changes in tau-PET we only selected subjects with a baseline tau-PET measurement plus at least one follow-up tau-PET scan. Other inclusion criteria for the present study were: (i) cognitively unimpaired or experiencing mild cognitive impairment[23]; (ii) a valid baseline measurement of CSF amyloid-β_{42}, amyloid-β_{40} and p-tau_{217} not more than 12 months from the baseline tau-PET scan (to determine tau biomarker profiles, see the 'Thresholds and grouping' section; Supplementary Table 1); (iii) no known genetic variants associated with autosomal dominant forms of neurodegenerative diseases (e.g. *APP*, *PSEN1* or *PSEN2* variants); and (iv) not a current or past participant in a clinical trial aimed at affecting the Alzheimer's disease pathological process. Participants were classified as having mild cognitive impairment if they performed worse than 1.5 standard deviations (SD) below the mean of controls on at least one of the cognitive domain(s) assessed according to age and education stratified test norms. The following domains were assessed; memory (immediate recall from the Alzheimer's Disease Assessment Scale-Cognition test), executive functions (Trail Making Test A and B and Symbol Digit Modalities Test), verbal ability (verbal fluency—animals and the 15-word short version of the Boston Naming Test) and visuospatial function (incomplete letters and cube analysis from the Visual Object and Space Perception battery). For a mild cognitive impairment diagnosis to be established, the observed cognitive impairment must not significantly interfere with independence in daily living, which is determined by a physician on the basis of a structured interview with the patient and an informant. Subjects that were not classified as having mild cognitive impairment were considered to be cognitively unimpaired.[22] We additionally included cognitively unimpaired, amyloid-β-negative individuals (aged >40

years), as a control group (see the 'Thresholds and grouping' section).

Standard protocol approvals, registrations and patient consents

All participants gave written informed consent. Ethical approval was given by the Regional Ethical Committee in Lund, Sweden. Approval for PET imaging was obtained from the Swedish Medical Products Agency and the local Radiation Safety Committee at Skåne University Hospital, Sweden.

Tau-PET

Detailed PET scanning procedures have been described previously.[21,24,25] Briefly, tau-PET scanning was performed using ^{18}F-RO948 on a digital Discovery MI scanner (GE Healthcare). Standardized uptake value ratio (SUVR) images were created using the 70–90 min post-injection interval and the inferior cerebellar cortex as reference region.[21,22,26] Each tau-PET SUVR image was rigidly co-reregistered to a high-resolution T_1- weighted MRI (Siemens3 T MAGNETOM Prisma) scan, performed a maximum of 6 months from the tau-PET scan. FreeSurfer (v.6.0, https://surfer.nmr.mgh.harvard.edu/) parcellation of the T_1-weighted MRI scan (see the 'MRI' section) was applied to the PET data to extract mean regional SUVR values that were used in region of interest analyses. We additionally obtained voxel-wise SUVRs by normalizing the MRI scans to MNI space using a standard statistical parametric mapping (SPM) 12-based pipeline[27] and then using the deformation fields calculated for normalization of the MRI scans to MNI space to also normalize the tau-PET SUVR images.

Composite regions of interest

Freesurfer-based regions were combined into three composite regions: an early region (entorhinal cortex; corresponding to Braak I/II), a temporal meta (intermediate)-region (amygdala, inferior/middle temporal gyri, fusiform gyrus and parahippocampal gyrus; corresponding to Braak III/IV)[28] and a late-stage region (corresponding to Braak V/VI; anterior cingulate, inferior frontal cortex, inferior parietal cortex, insular cortex, lateral occipital cortex, lingual gyrus, medial occipital cortex, middle frontal cortex, orbitofrontal cortex, paracentral cortex, precentral cortex, precuneus, postcentral cortex, posterior cingulate, superior frontal cortex, superior parietal cortex, superior temporal gyrus and supramarginal gyrus).[29,30]

Individual regions of interest

Given our hypothesis that isolated CSF p-tau positivity might predict the earliest stages of tau accumulation on tau-PET,[31,32] we also assessed tau-PET within individual regions that were recently identified to show a temporal order of abnormality in a tau-PET staging scheme.[33] The regions included in this staging scheme encompass early medial temporal lobe subregions (defined using automated segmentation of hippocampal subfields on T_1-weighted images[34]) as well as later-stage neocortical regions. Ordered according to the proposed temporal order of abnormality these regions are: entorhinal cortex, Brodmann area 35 (overlapping with the trans entorhinal cortex), anterior hippocampus, posterior hippocampus, Brodmann area 36, parahippocampal cortex, middle temporal cortex, inferior temporal cortex, inferior parietal cortex, isthmus cingulate cortex and precuneus.

CSF sampling and analysis

CSF samples were obtained using lumbar puncture performed within 12 months from the tau-PET scan. CSF p-tau$_{217}$ was assessed with the Lilly assay (Eli Lilly and Company) using the Meso Scale Discovery platform, as previously described.[11] CSF p-tau$_{217}$ was used rather than other CSF p-tau variants since it has been shown to be slightly better at detecting Alzheimer's disease tau pathology compared to other isoforms.[11] CSF concentrations of amyloid-β_{42} and amyloid-β_{40} were measured using the Roche NeuroToolKit on cobas e601 analyzers at the Clinical Neurochemistry Laboratory, University of Gothenburg, Sweden, as previously described.[35] Sampling and analysis procedures followed the Alzheimer's Association Flow Chart for CSF biomarkers.[36]

Thresholds and grouping

We performed Gaussian mixture modelling of CSF amyloid-β_{42}/amyloid-β_{40} ratios, CSF p-tau$_{217}$ and temporal meta-region SUVRs to determine cut-offs for abnormal CSF amyloid-β, CSF p-tau and tau-PET (Supplementary Fig. 1). The input for these models were the baseline measurements for each participant. Thresholds were determined to be <0.078 for amyloid-β_{42}/amyloid-β_{40} ratios, >110 pg/ml for CSF p-tau$_{217}$ and >1.40 SUVR for tau-PET (Supplementary Fig. 1A–C), and corresponded closely to thresholds used in previous publications.[21,30] Amyloid-β-positive participants were grouped into tau-negative (A+P–T–), tau-discordant (A+P+T–) and tau-positive (A+P+T+) groups. In accordance with studies showing that CSF p-tau positivity precedes tau-PET positivity in Alzheimer's disease,[15–17] there were no A+P–T+ individuals (Supplementary Fig. 1D). Amyloid-β-negative (A–), cognitively unimpaired participants were classified into a control group.

Cognition

Global cognition was assessed using the Mini-Mental State Examination (MMSE) and a modified preclinical Alzheimer cognitive composite [mPACC; consisting of the Alzheimer's Disease Assessment Scale (ADAS) delayed word recall (counted twice), animal fluency, Trail Making Test-B and MMSE].[37] For domain-specific impairments, we computed composite scores for memory (ADAS delayed word recall, ADAS immediate word recall-average across trials), executive functioning (Trail Making Test-B and Symbol Digit Substitution test), language (animal fluency and Boston Naming Test-average across trials) and visuospatial ability (Visual Object and Space Perception battery; cube and incomplete letters tests). Composite scores were calculated by first converting individual scores into z- scores based on the mean and standard deviation of the control individuals, and then averaging across tests within composite domains.

MRI

Detailed MRI acquisition protocols implemented in BioFINDER-2 are described in previous studies.[21,30] Briefly, T_1-weighted MRI was acquired on a 3 T MAGNETOM Prisma (Siemens Healthineers) scanner. Cortical reconstruction and volumetric segmentation were performed with the standard FreeSurfer (v.6.0) longitudinal image analysis pipeline (http://surfer.nmr.mgh.harvard.edu/). We computed cortical thickness in an early (entorhinal cortex), an intermediate 'AD-signature' (parahippocampal gyrus, inferior temporal, middle temporal, inferior parietal, fusiform and precuneus)[38] and a late composite region (temporoparietal cortex; superior

parietal, supramarginal, superior temporal, inferior temporal, banks of superior temporal sulcus, transverse temporal and temporal pole).

Statistical analyses

All statistical analyses and visualizations were performed in R v.4.0.3. Differences in demographics and clinical characteristics between groups were determined using general linear models with *post hoc* independent *t*-tests (for continuous variables) and χ^2-tests with *post hoc* Fisher's exact tests (for categorical variables). To obtain longitudinal changes in regional and voxel-wise tau-PET, regional cortical thickness and cognition we subtracted baseline values from the corresponding follow-up values, and then divided by the time interval. This yields a measure that indicates annual change in these measures. Longitudinal tau-PET was available for all subjects (by design; mean follow-up was 1.78 ± 0.19 years), cognitive follow-up was available for all but one subject (mean follow-up 2.18 ± 0.46 years) and follow-up MRI was available for 219/231 participants (95%; mean follow-up 1.74 ± 0.23 years; Supplementary Table 2). We used general linear models, which were adjusted for age, sex, clinical diagnosis at baseline (i.e. cognitively unimpaired or mild cognitive impairment) and (for cognition measures) education, to determine group differences in rates of annual change. Additionally, we performed Cox proportional hazard models, adjusted for age and sex, to assess group differences in clinical conversion rates (mean follow-up 2.12 ± 0.56 years), i.e. conversion to mild cognitive impairment for individuals who were cognitively unimpaired at baseline and conversion to dementia for individuals with mild cognitive impairment at baseline. A dementia diagnosis was based on the Diagnostic and Statistical Manual of Mental Disorders, Fifth Edition (DSM-5) criteria for major neurocognitive disorder due to probable Alzheimer's disease along with confirmation of abnormal amyloid accumulation according to the 2011 NIA-AA criteria for Alzheimer's disease dementia.[39] This means that a dementia diagnosis was established when an individual shows impairment in at least two cognitive domains and these impairments affect independence in activities of daily living, as established by a physician on the basis of a structured interview with the patient and an informant. For all effects, both uncorrected and Bonferroni-corrected *P*-values are reported.

Voxel-wise annual change maps were smoothed using a Gaussian kernel of 8 mm before being used in voxel-wise contrasts between groups. These contrasts were performed using the statistical parametric mapping software package version 12 implemented in MATLAB and adjusted for age, sex and baseline clinical diagnosis.

Data availability

Anonymized data will be shared by request from a qualified academic investigator for the sole purpose of replicating procedures and results presented in the article and as long as data transfer is in agreement with European Union legislation on the general data protection regulation and decisions by the Swedish Ethical Review Authority and Region Skåne, which should be regulated in a material transfer agreement.

Results

Demographic and clinical characteristics of the sample are displayed in Table 1. Our group classification of amyloid-β-positive (A+) individuals yielded 30 in the tau-negative (A+P−T−) group, 48 in the tau-discordant (A+P+T−; i.e. CSF p-tau-positive, tau-PET-negative) group and 18 in the tau-positive (A+P+T+) group (Supplementary Fig. 1D). The amyloid-β-negative (A−) cognitively unimpaired control group consisted of 135 individuals. Differences between the groups in demographics and clinical characteristics at baseline are provided in Supplementary Table 3. We found that age and *APOE*ε4 prevalence were higher, and education was lower, in the tau-discordant group than in the controls. Age and mild cognitive impairment prevalence were both lower in the tau-discordant group than in the tau-positive group. We found that baseline CSF p-tau$_{217}$, entorhinal tau and temporal meta-region tau were higher in the tau-discordant group than in the tau-negative and control groups, but all these measures were

Table 1 Baseline demographic and clinical characteristics

	Control (A−)	Tau-negative (A+P−T−)	Tau-discordant (A+P+T−)	Tau-positive (A+P+T+)
n	135	30	48	18
Age, years	64.6 (11.6)	69.1 (8.2)	71.1 (6.4)	75.3 (6.2)
Sex, male	66 (49)	12 (40)	26 (54)	10 (55)
Education, years	12.8 (3.4)	13.6 (3.6)	11.5 (3.6)	11.9 (3.6)
*APOE*ε4 prevalence	50 (37)	20 (67)	36 (75)	15 (83)
Diagnosis = MCI (%)	n.a.	10 (33)	13 (27)	13 (72)
Amnestic MCI (% of all MCI in group)	n.a.	6 (60)	9 (69)	10 (77)
Non-amnestic MCI (% of all MCI in group)	n.a.	4 (40)	4 (31)	3 (23)
CSF p-tau$_{217}$, pg/ml	44.2 (27.6)	72.3 (27.8)	232.8 (107.9)	395.8 (175.3)
Entorhinal tau, SUVR	1.12 (0.11)	1.13 (0.12)	1.34 (0.21)	1.77 (0.26)
Temporal meta-region, SUVR	1.15 (0.08)	1.15 (0.06)	1.21 (0.10)	1.70 (0.26)
Braak V/VI tau, SUVR	1.05 (0.08)	1.03 (0.06)	1.04 (0.08)	1.27 (0.19)
Entorhinal thickness, mm	3.32 (0.25)	3.14 (0.40)	3.19 (0.32)	2.75 (0.34)
AD-signature thickness, mm	2.44 (0.11)	2.40 (0.08)	2.41 (0.08)	2.28 (0.11)
Temporoparietal thickness, mm	1.71 (0.09)	1.68 (0.07)	1.69 (0.07)	1.61 (0.10)
MMSE	29.0 (1.2)	28.5 (1.9)	28.2 (1.5)	27.6 (2.1)
mPACC	0.0 (3.2)	−3.2 (4.3)	−3.8 (5.3)	−8.9 (5.0)

Values are mean (SD) for continuous variables and *n* (%) for categorical variables. MCI = mild cognitive impairment.

lower in the tau-discordant group than in the tau-positive group. In addition, baseline Braak V/VI tau was lower in the tau-discordant group compared to the tau-positive group. We also found that cortex in the entorhinal, AD-signature (intermediate) and late (temporoparietal) regions were all thinner at baseline in the tau-positive group than in the tau-discordant group, but there were no differences between the tau-discordant group and the control and tau-negative groups (Supplementary Table 3).

Differences in longitudinal changes in regional tau-PET

Yearly increases in tau-PET within the entorhinal cortex and within the temporal meta-region were faster in the tau-discordant group compared to both the tau-negative ($\beta = 0.030$, $P = 0.002$) and control ($\beta = 0.032$, $P = 0.000$) groups. Furthermore, yearly increases in tau within the Braak V/VI region were faster in the tau-discordant group compared to the tau-negative group ($\beta = 0.024$, $P = 0.000$). Yearly increases in tau-PET SUVR in the temporal meta-region and Braak V/VI region were slower in the tau-discordant group compared to the tau-positive group ($\beta = -0.067$, $P = 0.000$; $\beta = -0.035$, $P = 0.000$) but increases in entorhinal tau were not significantly different between these groups ($P = 0.697$; Fig. 1). Within individual regions based on a previously proposed tau staging scheme,[33] yearly increases in tau were found to be faster in the tau-discordant group than in the tau-negative and control groups across early (medial temporal lobe) and later stage (neocortical) regions but β-coefficients indicated more pronounced differences in early regions. *Post hoc* linear trend analyses assessing effect-size differences from the earlier to the later regions revealed a significant negative linear trend in effect sizes across regions when comparing the tau-discordant with the control group ($\beta = -0.0015$, $P < 0.001$) and when comparing the tau-discordant with the tau-negative group ($\beta = -0.0015$, $P < 0.001$). Furthermore, yearly increases in tau-PET in the tau-positive group were faster than in all the other groups, but these differences were more pronounced across later-stage regions (Fig. 2). The positive linear trend in effect-size differences across regions was significant when comparing the tau-positive with the tau-negative group ($\beta = 0.0068$, $P = 0.018$). This suggests that, in terms of tau accumulation stage, the tau-discordant group resides between the tau-negative and tau-positive groups. This is further highlighted by voxel-wise comparisons between the tau-discordant group and the other groups, showing that this group had faster tau accumulation rates in medial temporal lobe regions compared to control and tau-negative groups, while neocortical tau accumulation rates were faster in the tau-positive group than in the tau-discordant group (Fig. 3).

Differences in regional cortical thickness, cognition and clinical progression

Entorhinal cortical thickness decreased faster in the tau-discordant group compared to the control ($\beta = -0.025$, $P = 0.004$) group, but the same was true for the tau-negative ($\beta = -0.036$, $P = 0.000$) and tau-positive ($\beta = -0.050$, $P = 0.014$) groups (Fig. 4). Furthermore, there were no differences in global cognitive decline between the tau-discordant, tau-negative and control groups (all $P > 0.05$), but MMSE (versus control: $\beta = -0.776$, $P = 0.001$; versus tau-negative: $\beta = -0.542$, $P = 0.010$; versus tau-discordant: $\beta = -0.620$, $P = 0.002$) and mPACC (versus control: $\beta = -1.547$, $P = 0.001$; versus tau-negative: $\beta = -1.264$, $P = 0.010$; versus tau-discordant: $\beta = -1.253$, $P = 0.008$) scores declined faster in the tau-positive group compared to all other groups (Fig. 5). With regard to specific cognitive domains, there were no differences in longitudinal decline between the tau-discordant, tau-negative and control groups but longitudinal decline in memory (versus control: $\beta = -0.525$, $P = 0.001$; versus tau-negative: $\beta = -0.407$, $P = 0.012$; versus tau-discordant: $\beta = -0.407$, $P = 0.007$) and executive functions scores (versus controls: $\beta = -0.663$, $P = 0.001$; versus tau-negative: $\beta = -0.678$, $P = 0.001$; versus tau-discordant: $\beta = -0.633$, $P = 0.002$) were faster in the tau-positive

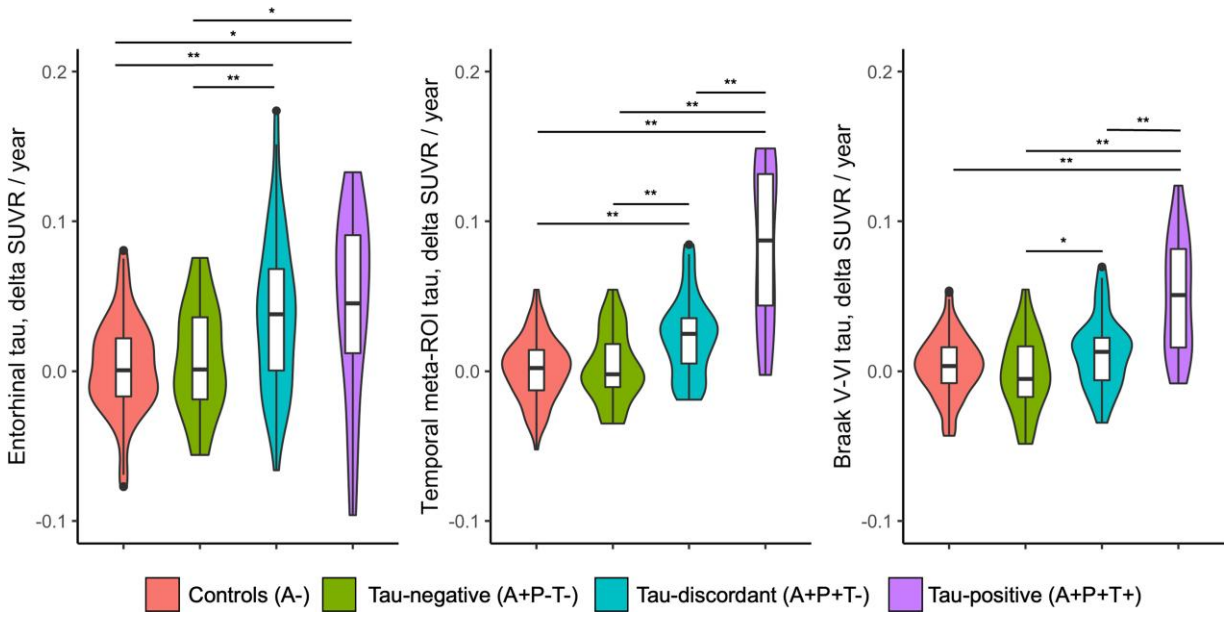

Figure 1 Differences in longitudinal change in tau-PET across composite regions of interest. Differences between groups were determined using general linear models adjusted for age, sex and clinical diagnosis. The box-and-whisker plots show median (thick horizontal lines within box), second and third quartile ranges (*bottom* and *top* of box) and the whiskers below and above each box show the first and fourth quartile range. The overlayed violin plots show the data distribution. *Difference at $P < 0.05$; **difference at $P < 0.05$, Bonferroni-corrected for six group comparisons. ROI = region of interest.

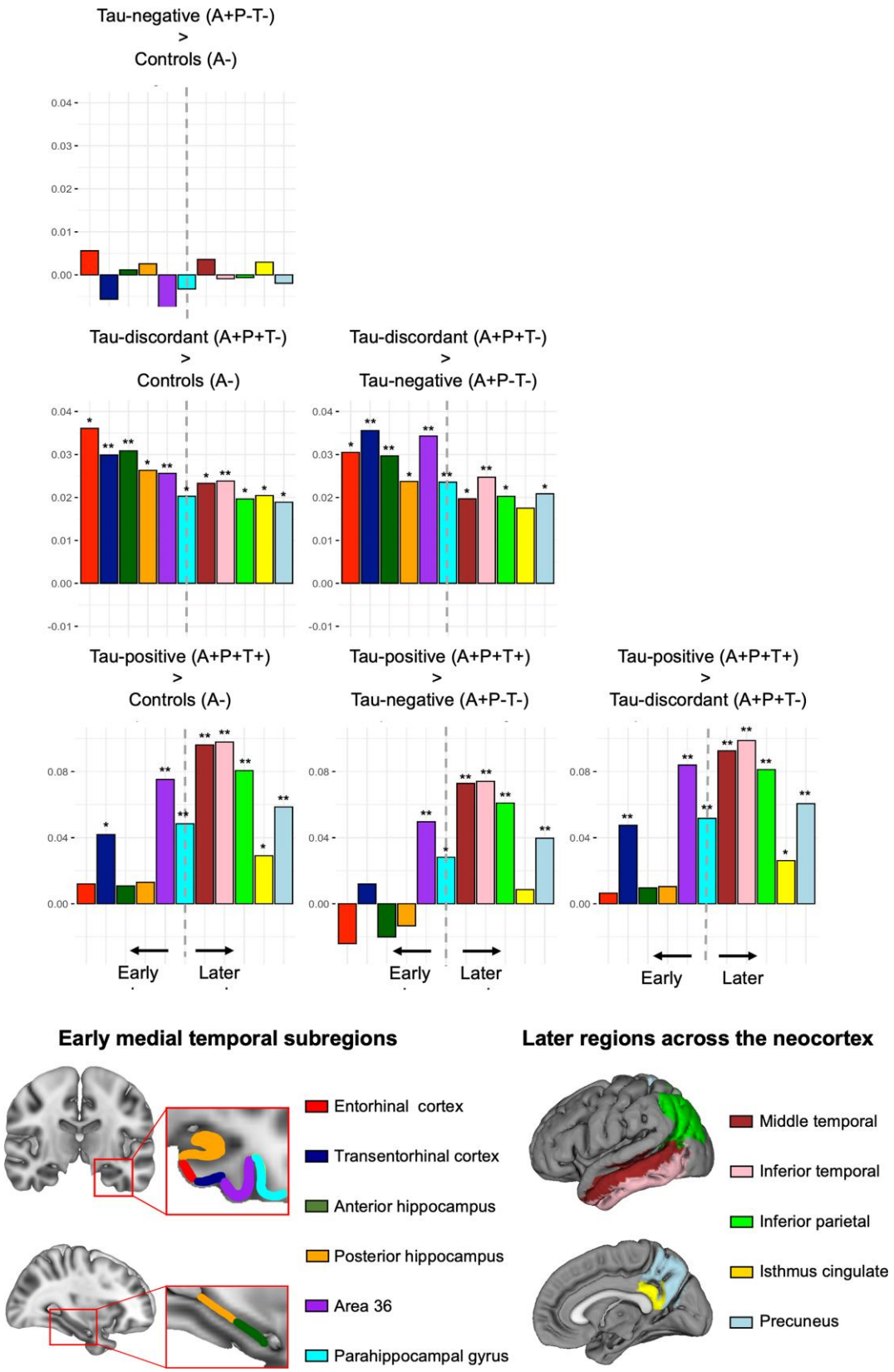

Figure 2 Differences in longitudinal change in regional tau-PET across staging regions of interest. Differences in yearly change in tau-PET between groups were determined using general linear models adjusted for age, sex and clinical diagnosis. The bars indicate beta coefficients representing the strength of the difference between groups in yearly change in tau-PET SUVR. All regions are based on staging regions from a previously determined tau-staging scheme (Berron *et al.*[33]), and, from left to right, run from early to late regions for tau accumulation. *Difference at $P < 0.05$; **difference at $P < 0.05$, Bonferroni-corrected for six group comparisons. Note that the *y*-axis has a different scale in the *bottom row*. Scales were selected to best visualize differences in effects across regions within a group comparison.

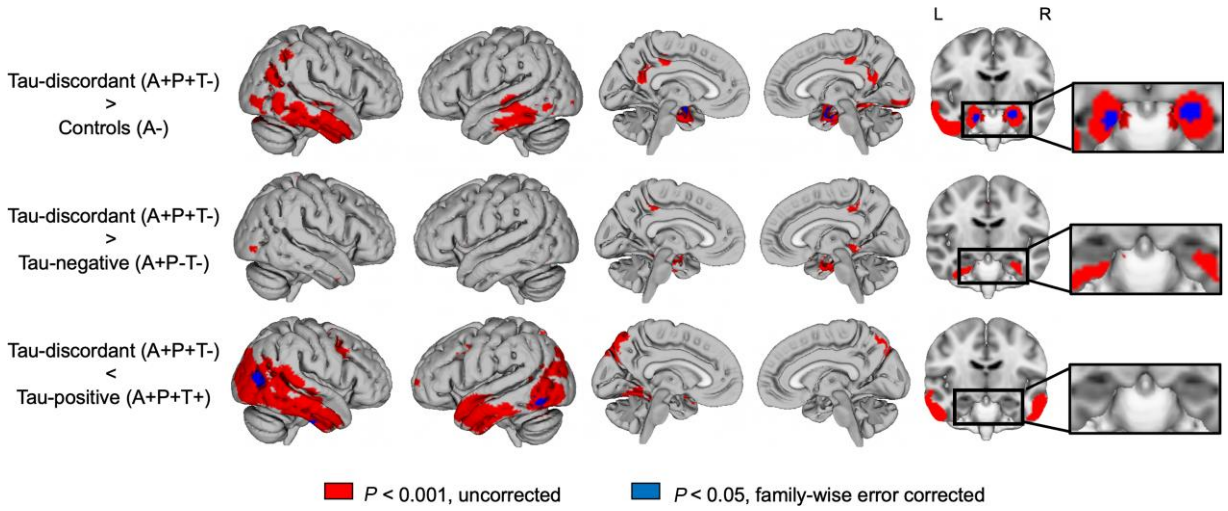

Figure 3 Voxel-wise comparisons of yearly change in tau-PET between groups. Contrasts were adjusted for age, sex and clinical diagnosis. Voxel-wise beta-maps, which are not dependent on sample sizes, are displayed in Supplementary Fig. 3.

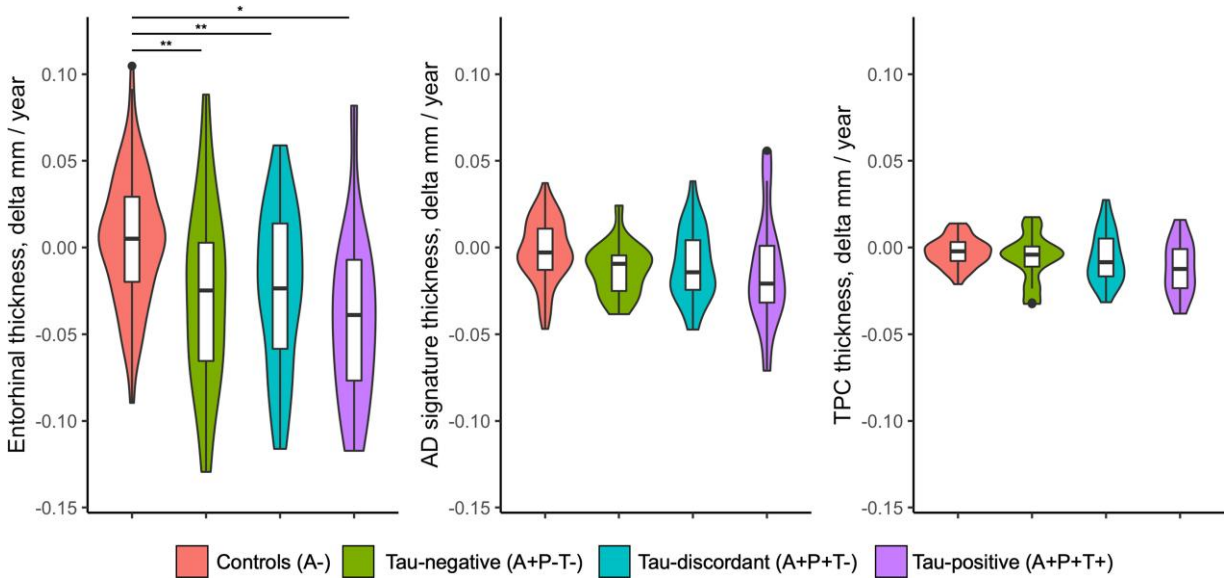

Figure 4 Differences in yearly change in regional cortical thickness. Differences between groups were determined using general linear models adjusted for age, sex, clinical diagnosis and (for cognition) education. The box plots indicate mean values and interquartile ranges and the overlaid violin plots show the data distribution. AD = Alzheimer's disease; TPC = temporoparietal cortex. *Difference at $P < 0.05$; **difference at $P < 0.05$ Bonferroni-corrected for six group comparisons.

group relative to the other groups. Furthermore, longitudinal decline in visuospatial scores were faster in the tau-discordant group compared to the control group ($\beta = -0.175$, $P = 0.008$) but this was also true for the tau-negative and tau-positive groups ($\beta = -0.198$, $P = 0.008$; $\beta = -0.256$, $P = 0.019$; Fig. 5). Cox proportional hazard models indicated a greater risk of clinical progression for the tau-discordant (hazard ratio = 2.23, 95% confidence interval = 0.07–4.40, $P = 0.043$) and tau-positive (hazard ratio = 2.95, 95% confidence interval = 0.83–5.08, $P = 0.001$) groups compared to the control group (reference group). Additionally, the tau-positive group had a greater risk of clinical progression compared to the tau-negative group (hazard ratio = 1.34, 95% confidence interval = 0.21–2.48, $P = 0.020$; Fig. 6).

Sensitivity analyses

As a sensitivity analysis, we additionally used Gaussian mixture models to determine a threshold for tau-PET positivity in the entorhinal cortex (SUVR = 1.38) and reclassified the groups using this region to define tau-PET+/–. Results obtained using these groups were very similar in terms of effect sizes to the main analyses and are provided in Supplementary Table 4. We also performed a sensitivity analysis whereby we define p-tau positivity using CSF p-tau$_{181}$ (performed at Eli Lilly and Company using the Meso Scale Discovery platform) and redefined the biomarker groups on the basis of this CSF p-tau$_{181}$ measure. Results obtained using these groups were similar to the main analyses using CSF p-tau$_{217}$ and are provided in Supplementary Table 5 . As an additional sensitivity

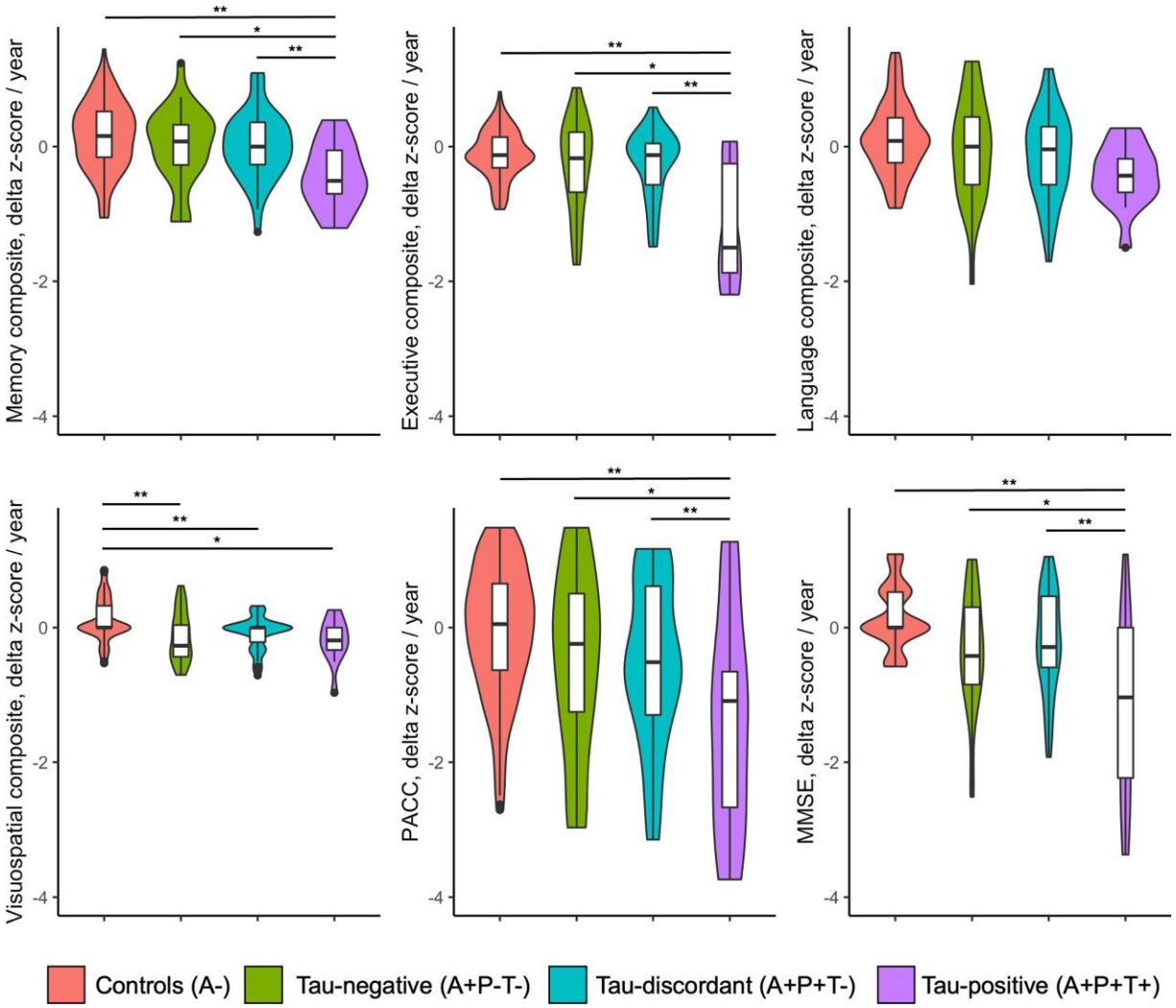

Figure 5 Differences in yearly change in cognition. Differences between groups were determined using general linear models adjusted for age, sex, clinical diagnosis and education. The box plots indicate mean values and interquartile ranges and the overlaid violin plots show the data distribution. *Difference at $P < 0.05$; **difference at $P < 0.05$ Bonferroni-corrected for six group comparisons.

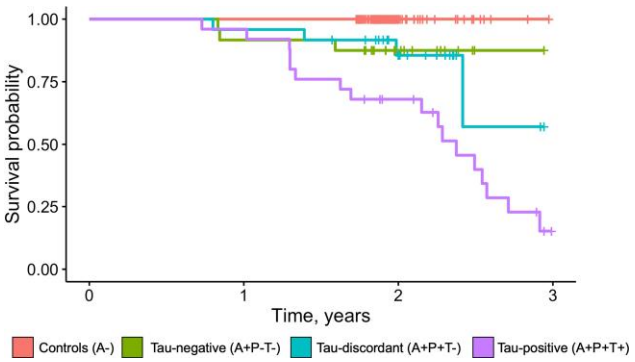

Figure 6 Differences in clinical progression. Differences between groups were determined using Cox proportional hazard models adjusted for age and sex. The Tau-discordant group had faster progression than controls. The Tau-positive group had faster progression than controls and the Tau-negative group.

analysis, we determined CSFp-tau$_{217}$ and tau-PET positivity by calculating 2.5 SD above the mean in the controls.[40] These thresholds [CSF p-tau$_{217}$ (110 pg/ml) and tau-PET (temporal meta-region SUVR = 1.35)] were similar to those obtained using Gaussian mixture models (i.e. the main analyses) and there was only a difference of two subjects who would have been reclassified into a different group (tau-discordant to tau-positive; Supplementary Fig. 1D). Given the almost complete overlap in groups between the two methods, we did not repeat all analyses using these alternative thresholds. Building on a previous observation that tau-PET is specifically related to posterior hippocampal volumes among cognitively unimpaired subjects from the BioFINDER-2 cohort,[41] we additionally assessed group differences in baseline and longitudinal posterior hippocampus volumes between groups and found that the tau-positive group had smaller baseline posterior hippocampus volumes, and also experienced faster decline in posterior hippocampus volumes, compared to controls ($\beta = -0.6334$, $P = 0.023$; $\beta = -0.243$, $P = 0.003$). We did not find any differences between the tau-discordant and the other groups (all $P > 0.05$). We also examined the effects of baseline CSF p-tau$_{217}$ on longitudinal tau-PET, cortical thickness and cognition in the tau-discordant group specifically using linear mixed model analyses. Similar to our main results, we found an effect of baseline CSF p-tau$_{217}$ on change over time in temporal meta-region tau and Braak V-VI tau (Time × CSF

p-tau$_{217}$ interaction effect, $\beta = 0.11$, $P < 0.001$; $\beta = 0.10$, $P < 0.01$), while there was no effect on change in cortical thickness (all $P > 0.05$). With regard to change in cognition, we found an effect on longitudinal change in memory (Time × CSF p-tau$_{217}$ interaction $\beta = -0.13$, $P < 0.001$) and language (Time × CSF p-tau$_{217}$ interaction $\beta = -0.14$, $P = 0.003$) indicating a worse decline with higher baseline CSF p-tau$_{217}$ levels.

Discussion

Among amyloid-β-positive (A+) individuals without dementia, we assessed the effect of isolated CSF p-tau positivity (P+) at subthreshold levels of tau-PET (T–) (i.e. A+P+T–, tau-discordant) on regional tau-PET, cortical thickness and cognition. Our main findings pointed to faster yearly tau increases in the A+P+T– group compared to both an A– control group and compared to an A+P–T– (i.e. concordant tau-negative) group. These differences were evident both in regions associated with early tau accumulation in the medial temporal lobe and in later regions in the neocortex, but were most pronounced in the early regions. Yearly increases in tau were faster in A+P+T+ (i.e. concordant tau-positive) compared to the A+P+T– group, and these differences were more pronounced in the later regions. This suggests that, among A+ individuals, those with an A+P+T– biomarker profile (p-tau-positive and tau-PET-negative) might reside in a tau stage between A+P–T– and A+P+T+ individuals. In contrast to our hypotheses, there was no indication that the A+P+T– group showed faster cortical thinning or accelerated cognitive decline compared to the A+P–T– group, but the A+P+T+ group consistently showed thinner cortex at baseline and faster cognitive decline compared to all other groups. We did, however, observe that the tau-discordant group had a greater risk of clinical progression compared to the control group, while the tau-negative group did not differ from the controls. Furthermore, sensitivity analyses using linear mixed-effects models in the tau-discordant group alone indicated a significant effect of baseline CSF p-tau$_{217}$ on decline in memory and language functions. These results suggest that p-tau positivity in isolation potentially affects cognitive decline but these effects are rather mild and should be interpreted with caution given the lack of an association with cognition in our primary analysis. Our findings collectively indicate that implementing a multi-modal approach to identify A+P+T– individuals yields a group that has faster tau accumulation than individuals who are A+P–T– and possibly an accelerated cognitive decline. This suggests that by targeting this A+P+T– group for future interventions one could halt increases in tau accumulation and prevent tau-related cognitive decline. In addition, given that tau accumulation in the A+P+T– group seems to be in the very earliest stages, this group also comprises an interesting group in which to study the mechanisms underlying the emergence and initial spread of tau pathology in Alzheimer's disease.

Biofluid measurements of tau pathology, such as CSF p-tau levels, have been proposed as cost-effective alternatives to tau-PET imaging, implying that measures of p-tau and tau-PET might be considered as interchangeable markers of tau pathology. Indeed, the 'T' (i.e. presence of tau) category in the AT(N) Alzheimer's disease biomarker classification system, could be defined by either CSF p-tau or tau-PET.[7] However, while this application of CSF p-tau could aid in identifying the presence of tau pathology in a clinical setting (e.g. to aid in differential diagnoses) an additional application of tau biomarkers is offered by multi-modal (CSF and PET) tau measurements, namely identifying individuals who are in the optimal window for intervention in the tau pathological process. Given that A+P+T– (tau-discordant) cases in the present study were shown to have increased tau accumulation compared to A+P–T– cases over a 2-year follow-up, interventions aimed at slowing the spread of tau would show higher treatment effect sizes in individuals with the tau-discordant biomarker profile compared to a group only selected on the basis of amyloid-β-positivity. In line with previous work indicating a close link between tau-PET and atrophy,[42] A+P+T+ cases (i.e. above threshold tau-PET) showed decreased cortical thickness already at the baseline visit. This indicates that these individuals have already experienced irreversible neurodegeneration, suggesting that the optimal window for intervention has passed. Individuals with a A+P+T– profile, residing on the tau pathological spectrum between the A+P–T– and A+P+T+ profiles, could therefore be considered to be in the Goldilocks zone for intervention, at a stage where tau has started accumulating (i.e. anti-tau treatment will probably have an effect) but where irreversible neurodegeneration is limited. A recent success story for considering the stage of tau pathology in clinical trials was provided in the phase II trial with the anti-amyloid-β antibody donanemab, which showed the highest effectiveness in individuals with intermediate levels of tau pathology as measured by tau-PET.[43] Implementing a multi-modal CSF and tau-PET approach to identify A+P+T– individuals could further fine-tune the selection of individuals into clinical trials based on tau biomarkers, maximizing the potential for treatment effects on tau pathology. One potential downside of implementing a multi-modal CSF and tau-PET approach is the considerable costs associated with tau-PET scans. However, given our findings that there were no individuals who were A+P–T+, the costs could be mitigated by pre-screening with biofluid (i.e. CSF or plasma analyses) and then administering PET scans only to those individuals who are A+P+.

Aside from foregoing the potential for clinical trial selection provided by multi-modal tau assessments, using CSF p-tau and tau-PET as interchangeable markers of tau pathology also ignores fundamental differences in what these biomarkers reflect. CSF p-tau reflects pathological processes in tau physiology, such as tau production, physiological neuronal release and clearance, hyperphosphorylation and increases in soluble tau levels as a result of neuronal damage.[15,44] For tau-PET, neuropathology studies have revealed that it mainly reflects aggregated tau proteins into neuritic tau and neurofibrillary tangles, especially in the later stages of Alzheimer's disease.[12,45,46] Indeed, it has been previously reported that CSF p-tau and tau-PET differentially affect atrophy and cognition,[47] with tau-PET being more strongly associated with both atrophy and cognition. These differences between p-tau and tau-PET align with the notion that CSF p-tau are reflective of a disease state (i.e. the presence of a pathological process), while tau-PET is reflective of disease stage (i.e. denoting the progression of the pathological process).[10,47,48] By implementing a multi-modal approach and leveraging the knowledge about what CSF and PET biomarkers for tau represent, one can better elucidate the mechanisms underlying the emergence and spread of tau pathology in Alzheimer's disease. Increasing our understanding of these processes may ultimately lead to the discovery of new drug targets to intervene in the tau pathological process.

Strengths of the current study include the multi-modal assessment of biomarkers for tau and relatively large sample size ($n = 231$) of subjects with longitudinal tau-PET, structural MRI and cognitive measures. The results of this study also need to be considered in light of some limitations. First, the selection of regions to define

tau-PET positivity comes with inherent limitations in terms of generalizing results to studies that use another region. However, sensitivity analyses revealed that our results are similar when using the entorhinal cortex rather than a temporal meta-region (i.e. the main analyses), which indicates that our findings are robust to region selection. The decision to present our main results using a temporal meta-region to determine tau-PET positivity was based on previous studies indicating that tau outside of the medial temporal lobe is a better predictor of progression in Alzheimer's disease as compared to entorhinal tau levels.[49] Furthermore, entorhinal tau is often seen in normal ageing,[50] and is not necessarily specific to individuals on the Alzheimer's disease continuum. Furthermore, we used thresholds to determine CSF p-tau and tau-PET positivity based on Gaussian mixture models, while others have previously used alternative methods,[40,49] hampering a direct comparison of our results to previous and possibly future study results. However, we showed that using an alternative method yielded very similar thresholds, which highlights that our grouping of biomarker profiles is robust to the method used to determine cut-offs. Similarly, we have used CSF p-tau$_{217}$ (and p-tau$_{181}$ in a sensitivity analysis) to define p-tau positivity but alternative measures, such as plasma p-tau biomarkers, may produce slightly different results. Also, since the sample sizes, were not sufficient to stratify the sample into cognitively unimpaired individuals and individuals with mild cognitive impairment, these two groups were pooled and we did not examine the differences between these diagnostic groups. This may have limited our ability to detect changes in cortical thickness and cognitive decline, which are expected to be greater in mild cognitively impaired individuals compared to cognitively unimpaired individuals. Future examinations in exclusively mild cognitively impaired subjects may show more pronounced effects of the tau-discordant biomarker profile on atrophy and cognitive decline. Similarly, our sample size was not sufficient to assess differential trajectories of tau-PET, cortical thickness and cognitive change between *APOEε4*-carriers and non-carriers. While *APOEε4* carriership has previously been shown to not affect longitudinal tau-PET change,[51] the potential effects of *APOEε4* on cognitive decline[52] warrants further investigation of the associations between *APOE* genotype and the A+P+T– biomarker profile. We also did not account for the possible confounding effects of co-pathologies such as vascular injury and TDP-43 deposition on longitudinal tau, atrophy and cognition between groups. Lastly, in our sample, 20% of subjects fell within the tau-discordant category but this prevalence may vary across cohorts. Future studies are needed to confirm prevalence estimates in alternative cohorts to inform numbers needed to screen to obtain sample sizes for clinical trials.

Biofluid p-tau and tau-PET are both incorporated as markers of tau pathology in the most recent research criteria for Alzheimer's disease,[7] and can both be used to define tau status in the amyloid, tau and neurodegeneration [AT(N)] classification system. However, our results indicate that it is prudent to split the 'T' category into measures of p-tau (P) and tau-PET (T) given that they partly measure different aspects of tau pathology and that p-tau typically becomes abnormal before tau-PET.[15,53] By implementing such an approach, we highlight that A+P+T– (amyloid-β positive, tau-discordant) cases show faster accumulation of tau than A+P–T– cases, while effects on neurodegeneration and cognitive decline were primarily detected in A+P+T+ cases. Taken together, while our findings indicate that isolated CSF p-tau positivity is only subtly related to cognitive decline, our results with regard to increased tau accumulation rated associated with the tau-discordant biomarker profile highlight that this group could provide an important target group for interventions against Alzheimer's disease pathology in the earliest phases. What is more, the tau-discordant biomarker profile could serve as a disease model to study the emergence and early spread of tau pathology in Alzheimer's disease.

Funding

This work was funded by ZonMW (project number 10510022110010) to Dr Colin Groot (PI), and by a European Research Council (ERC) research grant to Dr Rik Ossenkoppele (PI). Work at the authors' research centre was supported by the Swedish Research Council (2016-00906), the Knut and Alice Wallenberg foundation (2017-0383), the Marianne and Marcus Wallenberg foundation (2015.0125), the Strategic Research Area MultiPark (Multidisciplinary Research in Parkinson's disease) at Lund University, the Alzheimerfonden (AF-939932), the Swedish Brain Foundation (FO2021-0293), The Parkinsonfonden (1280/20), the Skåne University Hospital Foundation (2020-O000028), Regionalt Forskningsstöd (2020-0314) and the Swedish federal government under the ALF agreement (2018-Projekt0279). The precursor of ^{18}F-flutemetamol was sponsored by GE Healthcare. The precursor of ^{18}F-RO948 was provided by Roche. The funding sources had no role in the design and conduct of the study; in the collection, analysis, interpretation of the data; or in the preparation, review or approval of the manuscript.

Competing interests

S.P. has served on scientific advisory boards and/or given lectures in symposia sponsored by F. Hoffmann-La Roche, Biogen, Eli Lilly and Geras Solutions. R.O. has given lectures in symposia sponsored by GE Healthcare. O.H. has acquired research support (for the institution) from ADx, AVID Radiopharmaceuticals, Biogen, Eli Lilly, Eisai, Fujirebio, GE Healthcare, Pfizer and Roche. In the past 2 years, he has received consultancy/speaker fees from Amylyx, Alzpath, BioArctic, Biogen, Cerveau, Fujirebio, Genentech, Novartis, Roche and Siemens. The other authors report no disclosures. This study was supported by MultiPark—A Strategic Research Area at Lund University

Supplementary material

Supplementary material is available at *Brain* online.

References

1. Scheltens P, De Strooper B, Kivipelto M, *et al*. Alzheimer's disease. *Lancet*. 2021;397:1577-1590.
2. Hansson O. Biomarkers for neurodegenerative diseases. *Nat Med*. 2021;27:954-963.
3. Nelson PT, Alafuzoff I, Bigio EH, *et al*. Correlation of Alzheimer disease neuropathologic changes with cognitive status: A review of the literature. *J Neuropathol Exp Neurol*. 2012;71:362-381.
4. Ossenkoppele R, Schonhaut DR, Schöll M, *et al*. Tau PET patterns mirror clinical and neuroanatomical variability in Alzheimer's disease. *Brain*. 2016;139(Pt 5):1551-1567.
5. Leuzy A, Ashton NJ, Mattsson-Carlgren N, *et al*. 2020 Update on the clinical validity of cerebrospinal fluid amyloid, tau, and phospho-tau as biomarkers for Alzheimer's disease in the context of a structured 5-phase development framework. *Eur J Nucl Med Mol Imaging*. 2021;48:2121-2139.

6. Ossenkoppele R, Hansson O. Towards clinical application of tau PET tracers for diagnosing dementia due to Alzheimer's disease. *Alzheimers Dement*. 2021;17:1998-2008.
7. Jack CR Jr, Bennett DA, Blennow K, *et al*. NIA-AA research framework: Toward a biological definition of Alzheimer's disease. *Alzheimers Dement*. 2018;14:535-562.
8. Ossenkoppele R, Reimand J, Smith R, *et al*. Tau PET correlates with different Alzheimer's disease-related features compared to CSF and plasma p-tau biomarkers. *EMBO Mol Med*. 2021;13: e14398.
9. Mattsson N, Schöll M, Strandberg O, *et al*. 18 F-AV-1451 and CSF T-tau and P-tau as biomarkers in Alzheimer's disease. *EMBO Mol Med*. 2017;9:1212-1223.
10. La Joie R, Bejanin A, Fagan AM, *et al*. Associations between [(18)F] AV1451 tau PET and CSF measures of tau pathology in a clinical sample. *Neurology*. 2018;90:e282-e290.
11. Janelidze S, Stomrud E, Smith R, *et al*. Cerebrospinal fluid p-tau217 performs better than p-tau181 as a biomarker of Alzheimer's disease. *Nat Commun*. 2020;11:1683.
12. Fleisher AS, Pontecorvo MJ, Devous MD Sr., *et al*. Positron emission tomography imaging with [18F]flortaucipir and postmortem assessment of Alzheimer disease neuropathologic changes. *JAMA Neurol*. 2020;77:829-839.
13. Kuwabara H, Comley RA, Borroni E, *et al*. Evaluation of (18) F-RO-948 PET for quantitative assessment of tau accumulation in the human brain. *J Nucl Med*. 2018;59:1877-1884.
14. Xia CF, Arteaga J, Chen G, *et al*. [(18)F]T807, a novel tau positron emission tomography imaging agent for Alzheimer's disease. *Alzheimers Dement*. 2013;9:666-676.
15. Mattsson-Carlgren N, Andersson E, Janelidze S, *et al*. Aβ deposition is associated with increases in soluble and phosphorylated tau that precede a positive tau PET in Alzheimer's disease. *Sci Adv*. 2020;6:eaaz2387.
16. Barthélemy NR, Li Y, Joseph-Mathurin N, *et al*. A soluble phosphorylated tau signature links tau, amyloid and the evolution of stages of dominantly inherited Alzheimer's disease. *Nat Med*. 2020;26:398-407.
17. Reimand J, Collij L, Scheltens P, Bouwman F, Ossenkoppele R. Association of amyloid-β CSF/PET discordance and tau load 5 years later. *Neurology*. 2020;95:e2648-e2657.
18. De Wilde A, Reimand J, Teunissen CE, *et al*. Discordant amyloid-β PET and CSF biomarkers and its clinical consequences. *Alzheimers Res Ther*. 2019;11:78-78.
19. Mattsson N, Palmqvist S, Stomrud E, Vogel J, Hansson O. Staging β-amyloid pathology with amyloid positron emission tomography. *JAMA Neurol*. 2019;76:1319-1329.
20. Palmqvist S, Mattsson N, Hansson O. Cerebrospinal fluid analysis detects cerebral amyloid-β accumulation earlier than positron emission tomography. *Brain*. 2016;139(Pt 4): 1226-1236.
21. Leuzy A, Smith R, Ossenkoppele R, *et al*. Diagnostic performance of RO948 F 18 tau positron emission tomography in the differentiation of Alzheimer disease from other neurodegenerative disorders. *JAMA Neurol*. 2020;77:955-965.
22. Palmqvist S, Janelidze S, Quiroz YT, *et al*. Discriminative accuracy of plasma phospho-tau217 for Alzheimer disease vs other neurodegenerative disorders. *Jama*. 2020;324: 772-781.
23. Petersen RC, Smith GE, Waring SC, Ivnik RJ, Tangalos EG, Kokmen E. Mild cognitive impairment: Clinical characterization and outcome. *Arch Neurol*. 1999;56:303-308.
24. Smith R, Schöll M, Leuzy A, *et al*. Head-to-head comparison of tau positron emission tomography tracers [(18)F]flortaucipir and [(18)F]RO948. *Eur J Nucl Med Mol Imaging*. 2020;47:342-354.
25. Palmqvist S, Zetterberg H, Blennow K, *et al*. Accuracy of brain amyloid detection in clinical practice using cerebrospinal fluid β-amyloid 42: A cross-validation study against amyloid positron emission tomography. *JAMA Neurol*. 2014;71:1282-1289.
26. Smith R, Schöll M, Leuzy A, *et al*. Head-to-head comparison of tau positron emission tomography tracers [18 F]flortaucipir and [18 F]RO948. *Eur J Nucl Med Mol Imaging*. 2020;47:342-354.
27. Groot C, Sudre CH, Barkhof F, *et al*. Clinical phenotype, atrophy, and small vessel disease in APOE ϵ2 carriers with Alzheimer disease. *Neurology*. 2018;91:E1851-E1859.
28. Jack CR Jr, Wiste HJ, Weigand SD, *et al*. Defining imaging biomarker cut points for brain aging and Alzheimer's disease. *Alzheimers Dement*. 2017;13:205-216.
29. Cho H, Choi JY, Hwang MS, *et al*. In vivo cortical spreading pattern of tau and amyloid in the Alzheimer disease spectrum. *Ann Neurol*. 2016;80:247-258.
30. Ossenkoppele R, Rabinovici GD, Smith R, *et al*. Discriminative accuracy of [18F]flortaucipir positron emission tomography for Alzheimer disease vs other neurodegenerative disorders. *JAMA*. 2018;320:1151-1162.
31. Braak H, Braak E. Neuropathological stageing of Alzheimer-related changes. *Acta Neuropathol*. 1991;82:239-259.
32. Braak H, Thal DR, Ghebremedhin E, Del Tredici K. Stages of the pathologic process in Alzheimer disease. *J Neuropathol Exp Neurol*. 2011;70:960-969.
33. Berron D, Vogel JW, Insel PS, *et al*. Early stages of tau pathology and its associations with functional connectivity, atrophy and memory. *Brain*. 2021;144:2771-2783.
34. Xie L, Wisse LEM, Pluta J, *et al*. Automated segmentation of medial temporal lobe subregions on *in vivo* T1-weighted MRI in early stages of Alzheimer's disease. *Hum Brain Mapp*. 2019;40: 3431-3451.
35. Van Hulle C, Jonaitis EM, Betthauser TJ, *et al*. An examination of a novel multipanel of CSF biomarkers in the Alzheimer's disease clinical and pathological continuum. *Alzheimers Dement*. 2021;17:431-445.
36. Blennow K, Hampel H, Weiner M, Zetterberg H. Cerebrospinal fluid and plasma biomarkers in Alzheimer disease. *Nat Rev Neurol*. 2010;6:131-144.
37. Donohue MC, Sperling RA, Salmon DP, *et al*. The preclinical Alzheimer cognitive composite. *JAMA Neurol*. 2014;71:961-961.
38. Dickerson BC, Bakkour A, Salat DH, *et al*. The cortical signature of Alzheimer's disease: Regionally specific cortical thinning relates to symptom severity in very mild to mild AD dementia and is detectable in asymptomatic amyloid-positive individuals. *Cereb Cortex*. 2009;19:497-510.
39. McKhann GM, Knopman DS, Chertkow H, *et al*. The diagnosis of dementia due to Alzheimer's disease: recommendations from the National Institute on Aging-Alzheimer's Association workgroups on diagnostic guidelines for Alzheimer's disease. *Alzheimers Dement*. 2011;7:263-269.
40. Leuzy A, Janelidze S, Mattsson-Carlgren N, *et al*. Comparing the clinical utility and diagnostic performance of cerebrospinal fluid P-Tau181, P-Tau217 and P-Tau231 assays. *Neurology*. 2022;97:e1681-e1694;
41. Berron D, van Westen D, Ossenkoppele R, Strandberg O, Hansson O. Medial temporal lobe connectivity and its associations with cognition in early Alzheimer's disease. *Brain*. 2020; 143:1233-1248.
42. La Joie R, Visani AV, Baker SL, *et al*. Prospective longitudinal atrophy in Alzheimer's disease correlates with the intensity and topography of baseline tau-PET. *Sci Transl Med*. 2020;12: eaau5732.

43. Mintun MA, Lo AC, Duggan Evans C, *et al*. Donanemab in early Alzheimer's disease. *N Engl J Med*. 2021;384:1691-1704.
44. Jin M, Shepardson N, Yang T, Chen G, Walsh D, Selkoe DJ. Soluble amyloid beta-protein dimers isolated from Alzheimer cortex directly induce tau hyperphosphorylation and neuritic degeneration. *Proc Natl Acad Sci U S A*. 2011;108: 5819-5824.
45. Lowe VJ, Lundt ES, Albertson SM, *et al*. Tau-positron emission tomography correlates with neuropathology findings. *Alzheimers Dement*. 2020;16:561-571.
46. Smith R, Wibom M, Pawlik D, Englund E, Hansson O. Correlation of in vivo [18F]flortaucipir with postmortem Alzheimer disease tau pathology. *JAMA Neurol*. 2019;76:310-317.
47. Mattsson N, Schöll M, Strandberg O, *et al*. (18)F-AV-1451 and CSF T-tau and P-tau as biomarkers in Alzheimer's disease. *EMBO Mol Med*. 2017;9:1212-1223.
48. Blennow K, Hampel H. CSF markers for incipient Alzheimer's disease. *Lancet Neurol*. 2003;2:605-613.
49. Ossenkoppele R, Smith R, Mattsson-Carlgren N, *et al*. Accuracy of tau positron emission tomography as a prognostic marker in preclinical and prodromal Alzheimer disease: A head-to-head comparison against amyloid positron emission tomography and magnetic resonance imaging. *JAMA Neurol*. 2021;78:961-971.
50. Schöll M, Lockhart SN, Schonhaut DR, *et al*. PET imaging of tau deposition in the aging human brain. *Neuron*. 2016;89:971-982.
51. Smith R, Strandberg O, Mattsson-Carlgren N, *et al*. The accumulation rate of tau aggregates is higher in females and younger amyloid-positive subjects. *Brain*. 2020;143:3805-3815.
52. Jack CR, Wiste HJ, Weigand SD, *et al*. Predicting future rates of tau accumulation on PET. *Brain*. 2020;143:3136-3150.
53. Janelidze S, Berron D, Smith R, *et al*. Associations of plasma phospho-tau217 levels with tau positron emission tomography in early Alzheimer disease. *JAMA Neurol*. 2021;78:149-156.